DOI: 10.1002/cbic.200800408

Driving Force Analysis of Proton Tunnelling Across a Reactivity Series for an Enzyme-Substrate Complex

Parvinder Hothi,[a] Sam Hay,[a] Anna Roujeinikova,[a] Michael J. Sutcliffe,[b] Michael Lee,[c] David Leys,[a] Paul M. Cullis,[c] and Nigel S. Scrutton*[a]

Quantitative structure-activity relationships are widely used to probe C–H bond breakage by quinoprotein enzymes.[1–4] However, we showed recently that p*-substituted benzylamines are poor reactivity probes for the quinoprotein aromatic amine dehydrogenase (AADH) because of a requirement for structural change in the enzyme-substrate complex prior to C–H bond breakage.[5] This rearrangement is partially rate limiting, which leads to deflated kinetic isotope effects for* p*-substituted benzylamines. Here we report reactivity (driving force) studies of AADH with* p*-substituted phenylethylamines for which the kinetic isotope effect (~16) accompanying C–H/C–^{2}H bond breakage is elevated above the semi-classical limit. We show bond breakage occurs by quantum tunnelling and that within the context of the environmentally coupled framework for H-tunnelling the presence of the* p*-substituent places greater demand on the apparent need for fast promoting motions. The crystal structure of AADH soaked with phenylethylamine or methoxyphenylethylamine indicates that the structural change identified with* p*-substituted benzylamines should not limit the reaction with* p*-substituted phenylethylamines. This is consistent with the elevated kinetic isotope effects measured with* p*-substituted phenylethylamines. We find a good correlation in the rate constant for proton transfer with bond dissociation energy for the reactive C–H bond, consistent with a rate that is limited by a Marcus-like tunnelling mechanism. As the driving force becomes larger, the rate of proton transfer increases while the Marcus activation energy becomes smaller. This is the first experimental report of the driving force perturbation of H-tunnelling in enzymes using a series of related substrates. Our study provides further support for proton tunnelling in AADH.*

Introduction

The bacterial quinoprotein aromatic amine dehydrogenase (AADH) catalyses the oxidative deamination of aromatic amines using a tryptophan tryptophylquinone (TTQ) cofactor (Scheme 1).[6,7] In the reductive half-reaction (RHR), amine oxidation is accompanied by proton transfer from an iminoquinone intermediate derived from covalent addition of substrate to the TTQ centre (Figure 1). With tryptamine as a substrate, proton transfer occurs by environmentally coupled proton tunnelling, which is a reaction facilitated by a non-equilibrium and localised promoting motion in the iminoquinone intermediate.[8] The enzyme reaction cycle is completed by long-range electron transfer to the type 1 copper protein azurin following assembly of an AADH–azurin electron transfer complex.[9–11] Insight into the reaction cycle has come from detailed analysis of the crystal structures of reaction intermediates,[8,9,12] computational simulations of the reaction chemistry[8,13,14] and isotope analysis of the proton transfer step using fast reaction stopped-flow methods.[5,15,16] These studies have provided a detailed appreciation of the reaction chemistry, whilst emphasizing the importance of proton transfer by quantum tunnelling mechanisms (for example, with tryptamine substrate). Studies with other substrates (for example, *p*-substituted benzylamines) have revealed the need for structural reorganization prior to proton transfer.[5] This structural reorganization complicates analysis of the proton transfer step in studies of the temperature dependence of kinetic isotope effects (KIEs), which can be often used to infer tunnelling mechanisms.[17,18]

$$RCH_2NH_2 + H_2O \longrightarrow RCHO + NH_3 + 2e^- + 2H^+$$

Scheme 1. Reaction for the reduction of aromatic amines catalysed by AADH.

In principle, studies of quantitative structure-activity relationships (QSAR) are useful for inferring mechanistic information, particularly with quinoprotein enzyme systems.[3,4] With AADH, structural reorganization prior to bond breakage in studies with *p*-substituted benzylamines has prevented detailed mechanistic analysis, owing to steric clashes of the *p*-substituent

[a] *Dr. P. Hothi, Dr. S. Hay, Dr. A. Roujeinikova, Dr. D. Leys, Prof. N. S. Scrutton*
Manchester Interdisciplinary Biocentre, Faculty of Life Sciences
University of Manchester
131 Princess Street, Manchester M1 7DN (UK)
Fax: (+44) 161-306-8918
E-mail: nigel.scrutton@manchester.ac.uk

[b] *Prof. M. J. Sutcliffe*
Manchester Interdisciplinary Biocentre, School Chemical Engineering and Analytical Science, University of Manchester
131 Princess Street, Manchester M1 7DN (UK)

[c] *M. Lee, Prof. P. M. Cullis*
Department of Chemistry, University of Leicester
University Road, Leicester LE1 7RH (UK)

Supporting information for this article is available on the WWW under http://www.chembiochem.org or from the author.

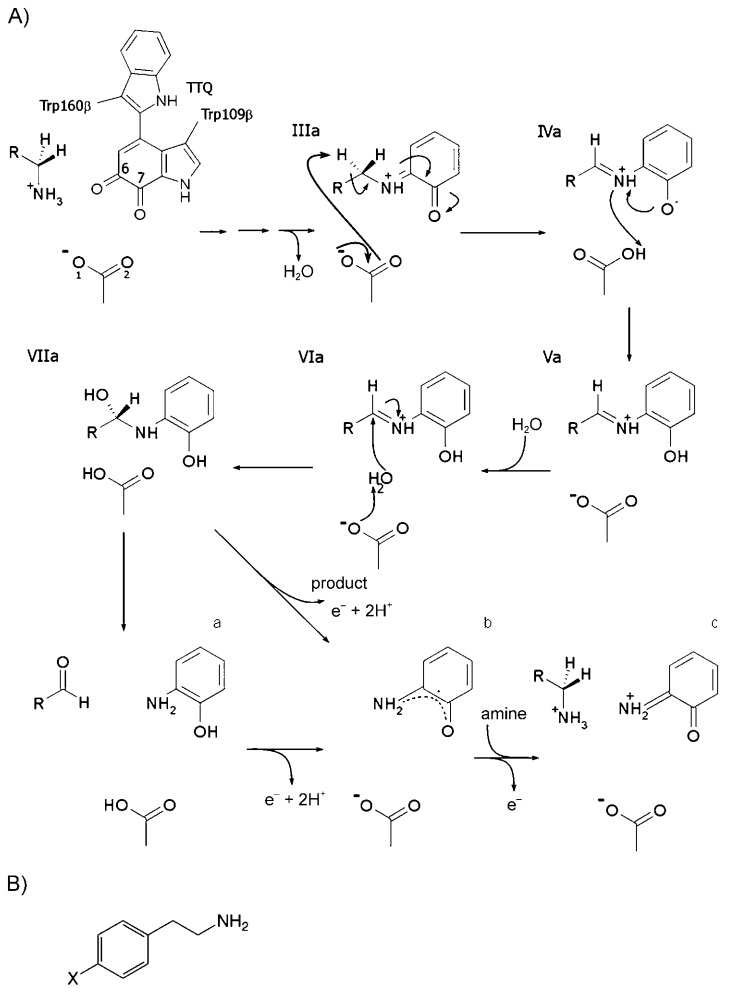

Figure 1. Reductive half-reaction of AADH with a generic amine substrate (A). Intermediates have been defined previously from crystallographic studies with tryptamine.[8] Intermediates are numbered with Roman numerals. Only key atoms are represented from intermediate II onward, whereas TTQ atoms C6 and C7 and Asp128β atoms O1 and O2 are labelled for intermediate I. A generic *para*-substituted phenylethylamine is also shown in panel B.

with residue Phe97α of the large AADH subunit.[5] This restriction is relieved upon the isolation of the small catalytic (TTQ-containing) subunit of AADH; this has facilitated QSAR analysis using Hammett methodology with *p*-substituted benzylamines.[16] Reactions of *p*-substituted benzylamines with the isolated small subunit are bimolecular and relatively slow, and it is not known if proton transfer is to Asp128β (the proton acceptor in native tetrameric AADH[8]) or to solvent. Unlike plots with native AADH, Hammett plots for the small subunit exhibit a strong correlation of structure-reactivity data with electronic substituent effects for reactions with *p*-substituted benzylamines and phenylethylamines and show that TTQ reduction is enhanced by electron withdrawing substituents.[16] We have been unable to demonstrate that proton transfer from the iminoquinone intermediate (formed between *p*-substituted benzylamines and the isolated subunit) to the unidentified proton acceptor occurs by quantum mechanical tunnelling.

In this paper, we report studies of native AADH in which we have employed a series of *p*-substituted phenylethylamines as reactivity probes. We conjectured that the additional methylene carbon in *p*-substituted phenylethylamines (compared with *p*-substituted benzylamines) would relieve any steric restriction on the reaction chemistry and thus facilitate detailed QSAR analysis of the reaction mechanism. We report 1) crystallographic analysis of AADH soaked with *p*-substituted phenylethylamines, 2) stopped-flow studies of the rate of C–H and C–^{2}H bond breakage, and 3) driving force analysis of the proton tunnelling reaction. The driving force analysis is consistent with proton transfer by quantum mechanical tunnelling. We also show an increased need for fast promoting motions as *p*-substituents are introduced ~6 Å away from the site of C–H bond breakage.

Results and Discussion

Crystal structures of AADH soaked with phenylethylamine or *p*-methoxyphenylethylamine

AADH crystals soaked with phenylethylamine or *p*-methoxyphenylethylamine rapidly change colour indicating full TTQ reduction. The crystal structure of a phenylethylamine soaked crystal that has been flash-cooled immediately following TTQ reduction reveals clear density in both active sites, corresponding to a covalent complex between phenylethylamine and TTQ (Figure 1). This was interpreted to represent the Schiff base intermediate V (intermediate terminology/numbering is according to ref. [8]) following the key proton abstraction by Asp128β and ensuing proton transfer steps to the TTQ O7. The structure is highly similar to the corresponding tryptamine intermediate V structure we reported previously[8] and reveals a similar angle is made between the Schiff base C=N bond and the TTQ aromatic plane. The substrate aromatic moiety is placed likewise in van der Waals contact between Phe97α and the peptide backbone amide connecting Val158β with Asn159β. In contrast, a *p*-methoxyphenylethylamine soaked crystal flash-cooled immediately following TTQ reduction reveals clear, but distinct electron density in both active sites from which the structures of the intermediates can be modelled (Figure 2). Both correspond to a covalent complex between *p*-methoxyphenylethylamine and TTQ, with one active site containing a Schiff base intermediate V, which is highly similar to that observed in the phenylethylamine soaked structure. The other active site contains the S-carbinolamine intermediate VII that is formed upon hydrolysis of intermediate V.[8] As observed for the phenylethylamine:AADH crystal structure, the *p*-methoxyphenylethylamine:AADH complexes are virtually identical to the corresponding tryptamine:AADH intermediate structures with obvious exception of the difference in substrate derived aromatic moiety.[8] The *p*-substituents of the various phenylethylamine derivatives can be easily accommodated by the active site cavity as demonstrated by the *p*-methoxyphenylethylamine:AADH complex

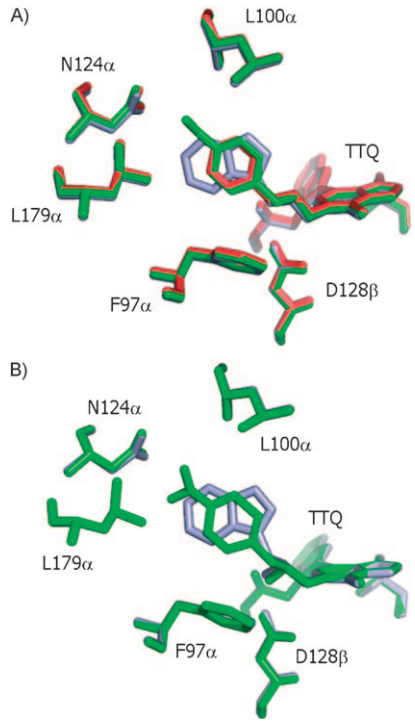

Figure 2. Crystal structures of AADH in complex with phenylethylamines. A) An active site overlay of the Schiff base intermediate V observed in phenylethylamine (red), *p*-methoxyphenylethylamine (green) and tryptamine (blue) soaked crystals. B) An active site overlay of the carbinolamine intermediate VII observed in *p*-methoxyphenylethylamine (green) and tryptamine (blue) soaked crystals. The *p* substituent in the former has multiple conformations. Numbering of reaction intermediates is as described previously.[8]

structure. In this case, the *p*-substituent is in close proximity of Leu100α, Asn124α and Leu179α, but none of these residues present any steric hindrance.

However, it should be noted that for the smaller aromatic amines, such as phenylethylamines, multiple positions for the aromatic moiety of the intermediate preceding the key hydrogen transfer from the substrate to Asp128β are possible.[12] Nevertheless, in the case of both tryptamine and the *p*-substituted phenylethylamine substrates, changes in the position of the key N1, C1, and C2 substrate derived atoms during catalysis appear not to significantly affect the position of the aromatic moiety. This contrasts markedly with the case for *p*-substituted benzylamine substrates, in which the C2 atom is part of the aromatic moiety itself and significant reorientation of the benzyl side chain (as well as several amino acid side chains) is required during catalysis.[5]

The reductive half-reaction of AADH with *p*-substituted phenylethylamines

Doubly deuterated phenylethylamines were synthesized as described in the Experimental Section and were > 95% chemically pure and 90-99% isotopically enriched, as judged from the ^{1}H high field NMR spectrum and integration of the residual N-CHD signal, respectively. Stopped-flow kinetic studies of the reductive half-reaction were performed as described in the Experimental Section. A large variation in the limiting rate constant for TTQ reduction was observed across the reactivity series, but little variation was observed in the H/D KIE (Table 1).

Table 1. Kinetic parameters determined from stopped-flow reactions of TTQ reduction in AADH with *p*-substituted phenylethylamines at 25 °C

p-substituent	k_{lim}^{H} [s^{-1}][a]	k_{lim}^{D} [s^{-1}][a]	KIE
H	45.6 ± 0.3	2.97 ± 0.03	15.4 ± 0.3
OH	412.7 ± 7.0	30.9 ± 0.25	13.4 ± 0.3
CH_3	44.7 ± 0.3	2.22 ± 0.01	20.1 ± 0.2
OCH_3	417.6 ± 11	26.4 ± 0.6	15.8 ± 0.5
NO_2	29.4 ± 0.2	1.77 ± 0.01	16.6 ± 0.2
F	93.1 ± 0.7	5.39 ± 0.04	17.3 ± 0.3
Cl	65.5 ± 0.3	3.25 ± 0.02	20.2 ± 0.2
Br	73.8 ± 0.3	3.76 ± 0.02	19.6 ± 0.2

[a] Observed rate constants at 200 μM (K_d < 5 μM) represent the limiting rates of TTQ reduction. For hydroxy- and methoxyphenylethylamines, kinetic parameters were determined by fitting data (observed rate of TTQ reduction versus concentration) with a standard hyperbolic expression. Experimental plots are available in Figure S1.

The reactions of most *p*-substituted phenylethylamines exhibited a lack of dependence on substrate concentration under pseudo-first-order conditions (Figure S1), and it was therefore assumed that K_d values were < 5 μM. For the reactions of phenylethylamines that exhibited a hyperbolic dependence on substrate concentration, the standard hyperbolic expression was used to determine K_d (9.5 ± 0.7 and 2.7 ± 0.2 μM for hydroxyl- and methoxyphenylethylamines, respectively, Figure S1).

Temperature analysis of reactions rates and KIEs

We analysed the temperature dependence of reaction rates with protiated and deuterated substrates to reveal tunnelling contributions to C–H and C–^{2}H bond breakage (Table 2). With

Table 2. Parameters obtained from temperature dependence studies of C–H and C–^{2}H bond breakage across the *p*-substituted phenylethylamine reactivity series.[a]

p-substituent	$\Delta H^{\ddagger H}$ [kJ mol^{-1}]	$\Delta H^{\ddagger D}$ [kJ mol^{-1}]	$\Delta\Delta H^{\ddagger}$ [kJ mol^{-1}]	A'^{H}: A'^{D}
H	55.2 ± 0.8	54.5 ± 0.9	0.7 ± 1.7	19.6 ± 0.5
OH	45.2 ± 1.3	51.5 ± 0.4	6.3 ± 1.7	0.86 ± 0.05
CH_3	58.8 ± 0.8	70.0 ± 0.8	11.2 ± 1.6	0.21 ± 0.01
OCH_3	44.2 ± 1.3	56.1 ± 0.6	11.9 ± 1.9	0.13 ± 0.01
NO_2	67.1 ± 1.3	72.6 ± 1.8	5.5 ± 3.1	2.12 ± 0.12
F	56.7 ± 0.9	63.7 ± 1.1	7.0 ± 2.0	0.97 ± 0.04
Cl	58.6 ± 0.6	69.4 ± 0.9	10.8 ± 1.5	0.26 ± 0.01
Br	59.6 ± 0.9	69.1 ± 0.9	9.5 ± 1.8	0.43 ± 0.01

[a] Reactions conducted in the temperature range 4–40 °C. Parameters were obtained by fitting to the Eyring equation. Reactions with protiated hydroxyl- and methoxyphenylethylamines were conducted over a more restricted temperature range (4–32 °C). Rate constants above this range were too fast to measure using the stopped-flow method.

phenylethylamine, the temperature dependence of the reaction rates ($\Delta H^{\ddagger H} = 54.7 \pm 0.6$ kJ mol^{-1}, $\Delta H^{\ddagger D} = 54.3 \pm 0.7$ kJ mol^{-1}) and associated KIE ($\Delta\Delta H^{\ddagger} = 0.7 \pm 1.7$ kJ mol^{-1}; Figure S2) is similar to those we have reported with tryptamine[8,15] ($\Delta H^{\ddagger H} = 57.3 \pm 3.4$ kJ mol^{-1}, $\Delta H^{\ddagger D} = 53.5 \pm 1.2$ kJ mol^{-1}; $\Delta\Delta H^{\ddagger} < 5$ kJ mol^{-1}), a substrate known to support tunnelling in AADH. Variation in the temperature dependence of KIEs is observed, however, across the *p*-substituted phenylethylamine series (Table 2). For all *p*-substituted phenylethylamines, the KIEs are temperature dependent ($\Delta\Delta H^{\ddagger} \sim 10 \pm 3$ kJ mol^{-1}; Figure S2).

Our previous work using tryptamine as substrate has established that proton transfer occurs by an environmentally coupled tunnelling reaction.[8,15] Within the environmentally coupled framework for H-tunnelling, a temperature dependent KIE indicates a role for non-equilibrium motions (promoting motions) in facilitating H-transfer.[17,19] We have reported the lack of a measurable temperature dependence of the KIE with tryptamine as a substrate,[8] but through numerical analysis we have also shown that this is consistent with the presence of a localised promoting motion of frequency (165 cm^{-1}), which is observed from spectral density analysis of motions from MD simulations.[13] The same explanation might be true for the apparent lack of a temperature dependence on the KIE with phenylethylamine. *p*-Substitution leads to a stronger temperature dependence, which suggests that promoting motions are more dominant with these susbtrates. In all cases, the large KIEs observed are inflated above the semi-classical limit. This contrasts with kinetic and structural data we have reported recently with a *p*-substituted benzylamine reactivity series (KIEs ~ 1), in which the reaction chemistry is limited by conformational change.[5] The elevated KIEs observed with the *p*-substituted phenylethylamines are consistent with a reaction geometry not impeded by conformational change (as seen with *p*-substituted benzylamine substrates) as inferred from the crystal structure of AADH with phenylethylamine and *p*-methoxyphenylethylamine (see above). The elevated KIEs, their temperature dependence and the Eyring prefactor ratios (A'^{H}:A'^{D}) therefore indicate that proton transfer occurs by environmentally coupled tunnelling across the *p*-substituted phenylethylamine reactivity series. Having established that the temperature dependence of the reaction rates and associated KIEs are consistent with an environmentally coupled tunnelling reaction, we now extend our analysis to investigate the driving force dependence of the observed reaction rates.

Driving force analysis of reaction rates

The rate of a proton tunnelling reaction can be calculated according to an extension of Marcus' electron transfer (ET) theory:[17,19–22]

$$k_{HT} \sim const \times e^{\frac{-\Delta G^{\ddagger}}{RT}} FC \times e^{\frac{-E_x}{RT}} \quad (1)$$

in which $\Delta G^{\ddagger}$ is the Marcus activation energy, *FC* is the Franck–Condon term that describes the nuclear wavefunction overlap of the reactant and product states, and E_X is the (gating) energy that confers the temperature-dependence of the KIE. The activation energy can be described by Eq. (2):

$$\Delta G^{\ddagger} = \frac{(\Delta G^0 + E_{vib} + \lambda)^2}{4\lambda} \quad (2)$$

where ΔG^0 is the driving force, E_{vib} is the change in vibrational energy of the transferred proton upon forming the product (see refs. [13], [17] for more details) and λ is the reorganization energy. A classical experimental validation of Marcus theory is the correlation of reaction rate with driving force.[20] For a proton transfer reaction, we would predict that, if Equation (1) is valid, 1) the rate of H-transfer will increase with increasing driving force, 2) the KIE will be nearly invariant with driving force, and 3) the enthalpy will decrease with increasing driving force. Please note that these predictions are not unique to Eq. 1 and similar dependencies would be expected for a purely classical transition state reaction. However, the magnitude of the KIEs ($\gg 7$) observed in this study preclude the use of transition state theory to model the AADH/phenylethylamine reaction. We should stress that while the enzyme community has largely been using the terms "promoting"- and "gating"-motions interchangeably, these motions are fast (ps) and non-equilibrated and in contrast to classical "gating" motions in ET reactions, which occur on long time scales and are rate-limiting. A test of "gated" ET is a driving force-independent rate of ET, whereas promoting vibrations will lead to a rate of H-transfer that *is* driving force (and temperature)-dependent.

For ET reactions, the driving force is varied by altering the electron affinity (reduction potentials) of either the donor or acceptor. For proton-transfer reactions, the analogous experiment involves the alteration of the proton affinity (that is, bond dissociation energy (BDE) or pK_a) of the proton donor or acceptor. If there is negligible entropy change during the reaction then[22]:

$$\Delta G^0_{PT} \approx BDE_{donor}\text{-}BDE_{acceptor} \quad (3)$$

Because the site of the transferred proton in phenylethylamine is removed from (that is, not conjugated with) the substituent/benzyl moiety (Figure 1), a Hammett-type analysis of the rate of proton transfer is not appropriate. Nevertheless, the *para* substituents will still have some effect on the BDE of the transferred proton. Because the proton-donor during the reductive half-reaction of AADH is a highly unstable iminoquinone intermediate species,[8] it is not possible to experimentally measure the pK_a/BDE of the proton donor. It is, however, possible to computationally determine the relevant BDE of the iminoquinone intermediate, and by calculating the BDE for each *p*-substituted phenylethylamine, we can estimate the effect of changing driving force on the reductive half-reaction of AADH. Note, we have not tried to calculate the actual BDEs or driving force in this study. Because the substituted phenylethylamines are not expected to greatly alter the BDE/pK_a of the aspartate proton acceptor, any change in driving force ($\Delta\Delta G^0$) should be proportional to the difference in BDE (ΔBDE) between the various substituted phenylethylamines. By nor-

malizing the BDEs we can investigate trends associated with change in rate with change in BDE while negating problems associated with systematic errors in the calculations or the pK_a shift associated with binding the phenylethylamine within the active site. These trends are qualitative only. We have estimated the BDE from semi-empirical (PM3) gas-phase calculations of the energy-minimized protonated and deprotonated *p*-phenylethylamine iminoquinone species. More extensive calculations on the whole enzyme are ongoing but require the solution of crystal structures of each of the AADH-bound substituted phenylethylamines. There is a reasonable correlation between the observed rate constants and ΔBDE (relative to unsubstituted phenylethylamine; Figure 3). An increase in iminoquinone BDE corresponds to a decrease in the driving force [Eq. (3)]. Therefore, the increase in rate with increasing driving force in Figure 2 is consistent with our predictions if the reaction is not in the Marcus inverted region.[20] We have previously estimated the reorganization energy for H-transfer during the reductive half-reaction of AADH with tryptamine to be very large (250–300 kJ mol^{-1}), making it very unlikely that $|\Delta G^0| > \lambda$ and therefore very unlikely that the reaction is in the inverted region. We have already shown that the KIE is fairly insensitive to *p*-substitution (Table 1) and thus to the driving force. While there is some change in the KIE with the differing substituents (Table 1), the difference is not particularly large. Further, because the temperature dependence of these KIEs is variable, it would appear that the involvement of the putative promoting motion[13] during this reaction differs for each substituent, in turn affecting both the temperature dependence and magnitude of the KIE. Finally, there is also a correlation between the apparent activation enthalpy and BDE (Figure 3), again consistent with our predictions. Together, these data provide good evidence that the proton transfer in AADH can be described by a Marcus-like mechanism, thereby lending additional support to inferences drawn from temperature dependent studies with AADH.

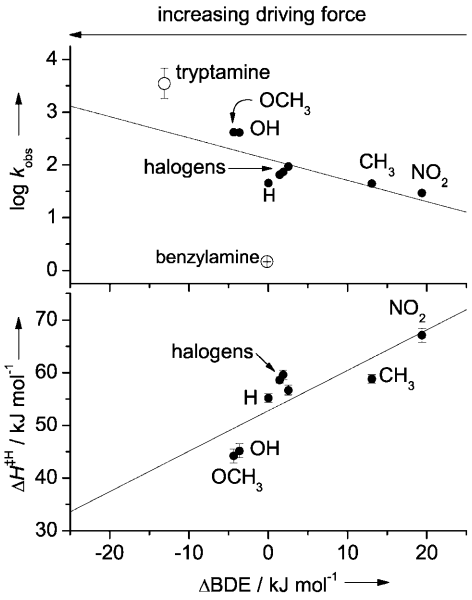

Figure 3. The pseudo-driving force dependence of the observed rate constant at 25 °C (top) and apparent enthalpy (bottom) of H-transfer during the reductive-half reaction of AADH with *p*-substituted phenylethylamine substrates. The solid lines are linear fits to the data with R^2 values of 0.58 (top) and 0.69 (bottom). The dependence with the observed rate with tryptamine and benzylamine are shown for reference. Note that the magnitude of the ΔBDE values may not reflect the magnitude of the change in the driving force experienced and it is only the trends that are important.

Conclusions

In this paper we have demonstrated that C–H bond breakage catalysed by AADH across a *p*-substituted phenylethylamine reactivity series is 1) not limited by conformational reorganisation, 2) occurs by quantum mechanical tunnelling and 3) has a driving force dependence consistent with the predictions of Marcus-like models for the reaction. Our work provides support for environmentally coupled H-tunnelling models that have been used previously to rationalise the temperature dependence of reaction rates and KIEs with a number of enzyme systems. Our work illustrates the utility of employing structurally related substrates to probe the driving force dependence of enzyme reactions. This provides an alternative approach to analyse enzymatic tunnelling reactions which complements the more traditional approaches that probe the effects of temperature variation on primary kinetic isotope effects.

Experimental Section

Materials: BisTris propane buffer, phenylethylamine, hydroxyphenylethylamine and nitrophenylethylamine were obtained from Sigma. Methyl-, fluoro- and chlorophenylethylamines were from Acros Organics (Loughborough, UK). Bromophenylethylamine was obtained from Fluorochem (Glossop, UK) and methoxyphenylethylamine from Apollo Scientific Ltd (Stockport, UK). Sodium borodeuteride (99% enriched) and deuterium oxide were obtained from Cambridge Isotope Laboratories (Nantwich, UK). The chemical purity of the deuterated reagents was determined to be >99% by high performance liquid chromatography, NMR, and gas chromatography, by the supplier.

Synthesis of dideuterated *p*-substituted phenethylamines: Dideuterated phenylethylamines were synthesized using a modification of the method reported by Umino et al.[23] (Figure S3), and as reported for dideuterated *p*-substituted benzylamines.[5] $NaBD_4$ (15 mmol) was suspended in dry THF (10 mL), TFA (15 mmol) in dry THF (5 mL) was added over 10 min at room temperature. The nitrile derivative (12.5 mmol) [each listed below] in dry THF (5 mL) was added to the mixture and stirred overnight. The reaction was quenched by the addition of D_2O (2 mL), water was added (ca. 20 mL), and the THF removed by rotary evaporation. The aqueous suspension was extracted with CH_2Cl_2, and the combined organic extracts were dried over solid Na_2SO_4 and filtered to give a solution of the free phenylethylamine in CH_2Cl_2. Addition of HCl-saturated CH_2Cl_2 to this solution precipitated the hydrochloride salt of the corresponding amine. Yields were typically 40–50%. Phenylethylamine HCl salts were >95% chemically pure and 90–99% isotopically enriched, as judged from the ^{1}H high field NMR spectrum and integration of the residual N-CHD signal, respectively. ^{1}H NMR spectra were recorded on a Bruker DPX300 NMR spectrometer. Mass

spectra were determined on a Micromass Quattro LC-MS (Elstree, UK) operating in electrospray mode and accurate mass positive ion FAB spectra were determined on a Kratos Concept spectrometer (Milton Keynes, UK).

Phenylethylamine HCl salt from reduction of phenylacetonitrile: ^{1}H NMR (300 MHz, CD_3OD): $\delta = 7.30$ (m, 5H), 2.96 (s, 2H), 3.16 (t, 5% H-C-D); MS: found *m/z* 194 [*M*−H(+2HCl)]. Accurate mass positive ion FAB calcd for $^{12}C_8H_{10}D_2N$ 124.10953, found *m/z* 124.10949.

4-Methylphenylethylamine HCl salt: ^{1}H NMR (CD_3OD): $\delta = 7.15$ (s, 4H), 2.91 (s, 2H), 2.31 (s, 3H), 3.13 (t, 5% H-C-D); MS: found *m/z* 208 [*M*−H(+2HCl)], 381 [2*M*−H(+3HCl)], 554 3*M*−H(+4HCl). Accurate mass positive ion FAB cacld for $^{12}C_9H_{12}D_2N$ 138.12518, found *m/z* 138.12513.

4-Methoxyphenylethylamine HCl salt: ^{1}H NMR (CD_3OD): $\delta = 7.19$ (d, 2H), 6.89 (d, 2H), 3.77 (s, 3H), 2.89 (s, 2H), 3.11 (t, 5% H-C-D); MS: found *m/z* 224 [*M*−H(+2HCl)], 413 [2*M*−H(+3HCl)], 602 [3*M*−H(+4HCl)]. Accurate mass positive ion FAB cacld for $^{12}C_9H_{12}D_2NO$ 154.12009, found *m/z* 154.12002.

4-Fluorophenylethylamine HCl salt: ^{1}H NMR (CD_3OD): $\delta = 7.29$ (m, 2H) 7.07 (m, 2H), 2.94 (s, 2H) 3.14 (t, 5% H-C-D); MS: found *m/z* 212 [*M*−H(+2HCl)], 389 [2*M*−H(+3HCl)], 566 [3*M*−H(+4HCl)]. Accurate mass positive ion FAB cacld for $^{12}C_8H_9D_2FN$ 142.10011, found *m/z* 142.10014.

4-Chlorophenylethylamine HCl salt: ^{1}H NMR (CD_3OD): $\delta = 7.35$ (d, 2H), 7.28 (d, 2H), 2.95 (s, 2H), 3.16 (t, 5% H-C-D); MS: found *m/z* 228 [*M*−H(+2HCl)], 421 [2*M*−H(+3HCl)], 614 [3*M*−H(+4HCl]. Accurate mass positive ion FAB cacld for $^{12}C_8H_9D_2ClN$ 158.07056, found *m/z* 158.07052.

4-Bromophenylethylamine HCl salt: ^{1}H NMR (CD_3OD): $\delta = 7.50$ (d, 2H), 7.22 (d, 2H), 2.93 (s, 2H), 3.15 (10% H-C-D, t); MS: found *m/z* 185 [*M*−NH_2]. Accurate mass positive ion FAB cacld for $^{12}C_8H_9D_2BrN$ 202.02004, found *m/z* 202.02001.

4-Nitrophenylethylamine HCl salt: ^{1}H NMR (CD_3OD): $\delta = 8.22$ (d, 2H), 7.55 (d, 2H), 3.11 (s, 2H), 3.21 (2% H-C-D, t); MS: found *m/z* 239 [*M*−H(+2HCl)], 443 [2*M*−H(+3HCl)]. Accurate mass positive ion FAB cacld for $^{12}C_8H_9D_2N_2O_2$ 169.09461, found *m/z* 9.09457.

4-Hydroxyphenylethylamine HCl salt: ^{1}H NMR (CD_3OD): $\delta = 7.08$ (d, 2H),6.77 (d, 2H),2.84 (s, 2H), 3.09 (12% H-C-D, t); MS: 174 [*M*−H-(+HCl)], 385 [2*M*−H(+3HCl)]. Accurate mass positive ion FAB cacld for $^{12}C_8H_{10}D_2NO$ 140.10444, found *m/z* 140.10440. In all cases, *M* is the mass of the free amine.

Purification of enzyme: AADH was isolated from *Alcaligenes faecalis* IFO 14479[24] and purified as described previously.[7] Prior to use in kinetic studies, AADH was reoxidized with potassium ferricyanide and exchanged into the required buffer (10 mM bis-tris propane, pH 7.5) by gel exclusion chromatography. Enzyme concentration was determined using an extinction coefficient of 27600 $M^{-1}cm^{-1}$ at 433 nm.[6]

Stopped-flow kinetic studies of the reductive half-reaction: Rapid kinetic studies were performed by using an Applied Photophysics SX.18MV stopped-flow spectrophotometer (Leatherhead, UK). Oxidized AADH (reaction cell concentration 1 μM) in bis-tris propane buffer (10 mM, pH 7.5), was rapidly mixed with various concentrations of substrate (see Results), at 25 °C. Reduction of the TTQ cofactor was followed at 456 nm. Data were analyzed by nonlinear least squares regression analysis on an Acorn RISC PC using Spectrakinetics software (Applied Photophysics). For each substrate concentration, at least three replica measurements were collected and averaged, each containing 1000 data points. Under pseudo-first-order conditions, absorbance changes accompanying enzyme reduction were monophasic or biphasic in nature (k_1, >85% of the total amplitude change) and were analyzed by fitting to the standard single or double exponential expression, respectively. Where appropriate, the concentration dependence of k_{obs} was analyzed by fitting to the standard hyperbolic expression[25] to obtain values for the apparent dissociation constant for the enzyme-substrate complex, K_d, and the limiting rate, k_{lim}, of TTQ reduction. In temperature dependence studies, enzyme was equilibrated in the stopped-flow apparatus at the appropriate temperature prior to the acquisition of kinetic data. Temperature control was achieved using a thermostatic circulating water bath, and the temperature was monitored directly in the stopped-flow apparatus using a semiconductor sensor. Control studies of the concentration dependence of bond cleavage at 4 °C and 40 °C, for all *p*-substituted phenylethylamines, indicated that the K_d was not substantially perturbed on changing temperature. Thermodynamic parameters were obtained by fitting data to the Eyring equation.

Crystallography: AADH crystals were obtained as described before.[8] Crystals were soaked in mother liquor supplemented with phenylethylamine or *p*-methoxyphenylethylamine (50 mM) and flash-cooled in liquid nitrogen immediately following complete reduction of the TTQ. Data were collected at ID14 beamlines at the European Synchrotron Radiation Facility (ESRF), Grenoble, France. Structures were refined using refmac5[26] with final refinement statistics Table S2.

Computational methods: The bond dissociation energy was estimated from the difference in the heat of formation of the energy-minimized protonated and deprotonated iminoquinone species calculated using Parametric method 3 (PM3)[27] in the gas phase (Figure S4). Calculations were made using either Gaussian 03[28] or Arguslab 4.01.[29]

Abbreviations: AADH, aromatic amine dehydrogenase; BDE, bond dissociation energy; BisTris, bis(2-hydroxyethyl)iminotris(hydroxymethyl)methane; ET, electron transfer; KIE, kinetic isotope effect; TTQ, tryptophan tryptophylquinone; CH_2Cl_2, dichloromethane; $NaBD_4$, sodium borodeuteride; Na_2SO_4, anhydrous sodium sulfate; TFA, trifluoroacetic acid; THF, tetrahydrofuran.

Acknowledgements

This work was funded by the UK Biotechnology and Biological Sciences Research Council. D.L. is a Royal Society University Research Fellow. N.S.S. is a BBSRC Professorial Fellow.

Keywords: amine oxidation · enzyme catalysis · isotope effects · proton tunnelling · quinoprotein

[1] V. L. Davidson, L. H. Jones, M. E. Graichen, *Biochemistry* **1992**, *31*, 3385.
[2] Y. L. Hyun, V. L. Davidson, *Biochemistry* **1995**, *34*, 816.
[3] P. R. Williamson, H. M. Kagan, *J. Biol. Chem.* **1987**, *262*, 14520.
[4] C. Hartmann, J. P. Klinman, *Biochemistry* **1991**, *30*, 4605.
[5] P. Hothi, A. Roujeinikova, K. Abu Khadra, M. Lee, P. Cullis, D. Leys, N. S. Scrutton, *Biochemistry* **2007**, *46*, 9250.
[6] S. Govindaraj, E. Eisenstein, L. H. Jones, J. Sanders-Loehr, A. Y. Chistoserdov, V. L. Davidson, S. L. Edwards, *J. Bacteriol.* **1994**, *176*, 2922.
[7] P. Hothi, K. A. Khadra, J. P. Combe, D. Leys, N. S. Scrutton, *FEBS J.* **2005**, *272*, 5894.

[8] L. Masgrau, A. Roujeinikova, L. O. Johannissen, P. Hothi, J. Basran, K. E. Ranaghan, A. J. Mulholland, M. J. Sutcliffe, N. S. Scrutton, D. Leys, *Science* **2006**, *312*, 237.
[9] A. Roujeinikova, N. S. Scrutton, D. Leys, *J. Biol. Chem.* **2006**, *281*, 40264.
[10] N. Sukumar, Z. W. Chen, D. Ferrari, A. Merli, G. L. Rossi, H. D. Bellamy, A. Chistoserdov, V. L. Davidson, F. S. Mathews, *Biochemistry* **2006**, *45*, 13500.
[11] Y. L. Hyun, V. L. Davidson, *Biochemistry* **1995**, *34*, 12249.
[12] A. Roujeinikova, P. Hothi, L. Masgrau, M. J. Sutcliffe, N. S. Scrutton, D. Leys, *J. Biol. Chem.* **2007**, *282*, 23766.
[13] L. O. Johannissen, S. Hay, N. S. Scrutton, M. J. Sutcliffe, *J. Phys. Chem. B* **2007**, *111*, 2631.
[14] L. O. Johannissen, N. S. Scrutton, M. J. Sutcliffe, *J. R. Soc. Interface* **2008**, DOI: 10.1098/rsif.2008.0068.focus.
[15] J. Basran, S. Patel, M. J. Sutcliffe, N. S. Scrutton, *J. Biol. Chem.* **2001**, *276*, 6234.
[16] P. Hothi, M. Lee, P. M. Cullis, D. Leys, N. S. Scrutton, *Biochemistry* **2008**, *47*, 183.
[17] M. J. Knapp, J. P. Klinman, *Eur. J. Biochem.* **2002**, *269*, 3113.
[18] M. J. Sutcliffe, N. S. Scrutton, *Eur. J. Biochem.* **2002**, *269*, 3096.
[19] L. Masgrau, J. Basran, P. Hothi, M. J. Sutcliffe, N. S. Scrutton, *Arch. Biochem. Biophys.* **2004**, *428*, 41.
[20] R. A. Marcus, N. Sutin, *Biochim. Biophys. Acta* **1985**, *811*, 265.
[21] A. M. Kuznetsov, J. Ulstrup, *Can. J. Chem.* **1999**, *77*, 1085.
[22] M. J. Knapp, K. Rickert, J. P. Klinman, *J. Am. Chem. Soc.* **2002**, *124*, 3865.
[23] N. Umino, T. Iwakuma, N. Itoh, *Tetrahedron Lett.* **1976**, *17*, 2875.
[24] M. Iwaki, T. Yagi, K. Horiike, Y. Saeki, T. Ushijima, M. Nozaki, *Arch. Biochem. Biophys.* **1983**, *220*, 253.
[25] S. Strickland, G. Palmer, V. Massey, *J. Biol. Chem.* **1975**, *250*, 4048.
[26] G. N. Murshudov, A. A. Vagin, E. J. Dodson, *Acta Crystallogr. D Biol. Crystallogr.* **1997**, *53*, 240.
[27] J. J. P. Stewart, *J. Comp. Chem.* **1989**, *10*, 209.
[28] M. J. Frisch, G. W. Trucks, H. B. Schlegel, G. E. Scuseria, M. A. Robb, J. R. Cheeseman, J. Montgomery, J. A., T. Vreven, K. N. Kudin, J. C. Burant, J. M. Millam, S. S. Iyengar, J. Tomasi, V. Barone, B. Mennucci, M. Cossi, G. Scalmani, N. Rega, G. A. Petersson, H. Nakatsuji, M. Hada, M. Ehara, K. Toyota, R. Fukuda, J. Hasegawa, M. Ishida, T. Nakajima, Y. Honda, O. Kitao, H. Nakai, M. Klene, X. Li, J. E. Knox, H. P. Hratchian, J. B. Cross, V. Bakken, C. Adamo, J. Jaramillo, R. Gomperts, R. E. Stratmann, O. Yazyev, A. J. Austin, R. Cammi, C. Pomelli, J. W. Ochterski, P. Y. Ayala, K. Morokuma, G. A. Voth, P. Salvador, J. J. Dannenberg, V. G. Zakrzewski, S. Dapprich, A. D. Daniels, M. C. Strain, O. Farkas, D. K. Malick, A. D. Rabuck, K. Raghavachari, J. B. Foresman, J. V. Ortiz, Q. Cui, A. G. Baboul, S. Clifford, J. Cioslowski, B. B. Stefanov, G. Liu, A. Liashenko, P. Piskorz, I. Komaromi, R. L. Martin, D. J. Fox, T. Keith, M. A. Al-Laham, C. Y. Peng, A. Nanayakkara, M. Challacombe, P. M. W. Gill, B. Johnson, W. Chen, M. W. Wong, C. Gonzalez, J. A. Pople, Gaussian, Inc., Wallingford CT, **2004**.
[29] M. A. Thompson, Planaria Software LLC, Seattle, WA.

Received: June 16, 2008

